Supporting Information

Effect of Concentration on the Electrochemistry and Speciation of the Magnesium Aluminum Chloride Complex Electrolyte Solution

*Kimberly A. See, Yao-Min Liu, Yeyoung Ha, Christopher J. Barile, Andrew A. Gewirth**

Department of Chemistry, University of Illinois at Urbana-Champaign, Urbana, Illinois 61801 United States

AUTHOR INFORMATION

Corresponding Author

*Andrew A. Gewirth, agewirth@illinois.edu

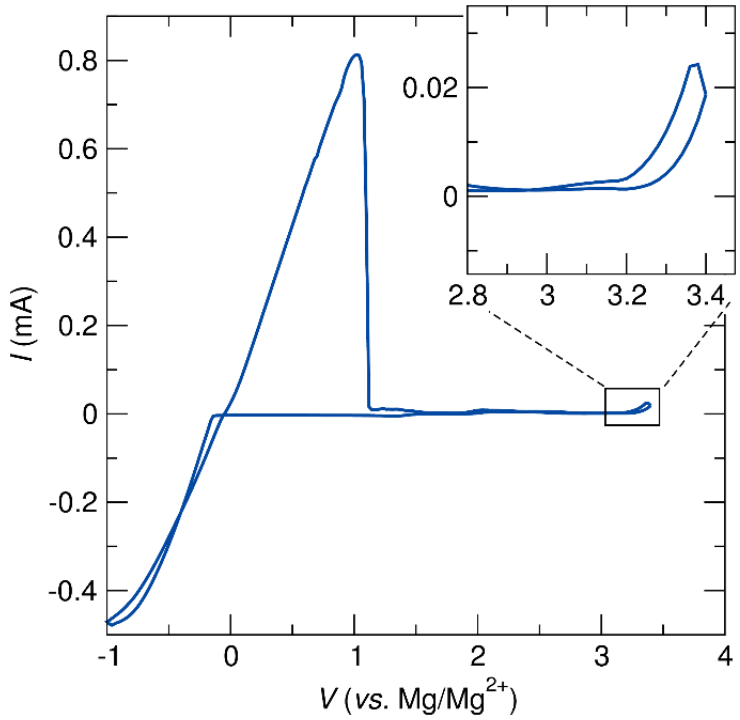

Figure S1. Cyclic voltammogram of the high concentration MACC electrolyte (0.3 M $MgCl_2$ + 0.15 M $AlCl_3$) from −1 V to 3.4 V (vs. Mg/Mg^{2+}) at 5 mV s^{-1} on a Pt working electrode with a Mg counter/reference. The high concentration MACC maintains an anodic stability up to 3.2 V (vs. Mg/Mg^{2+}) as shown by the inset.

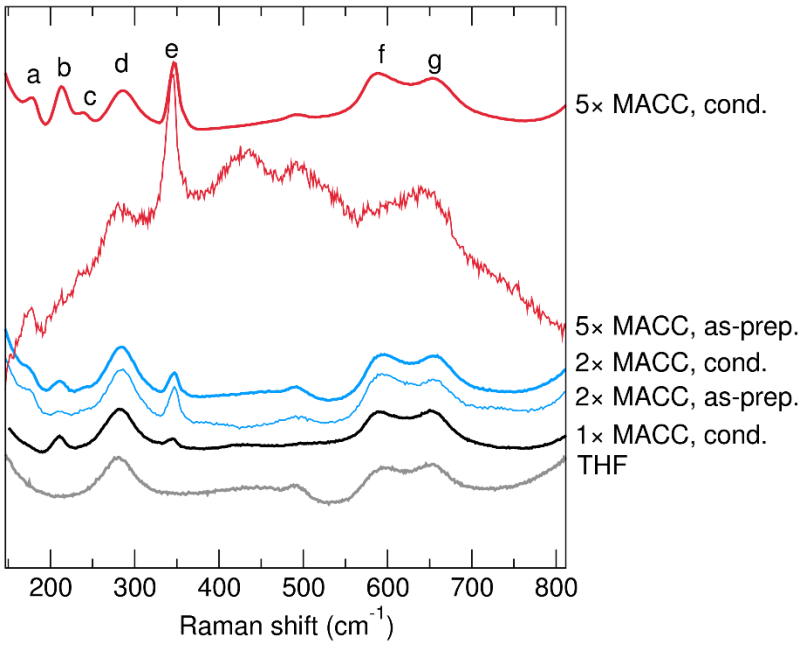

Figure S2. Raman spectra of the as-prepared and conditioned 2× and 5× MACC electrolytes.

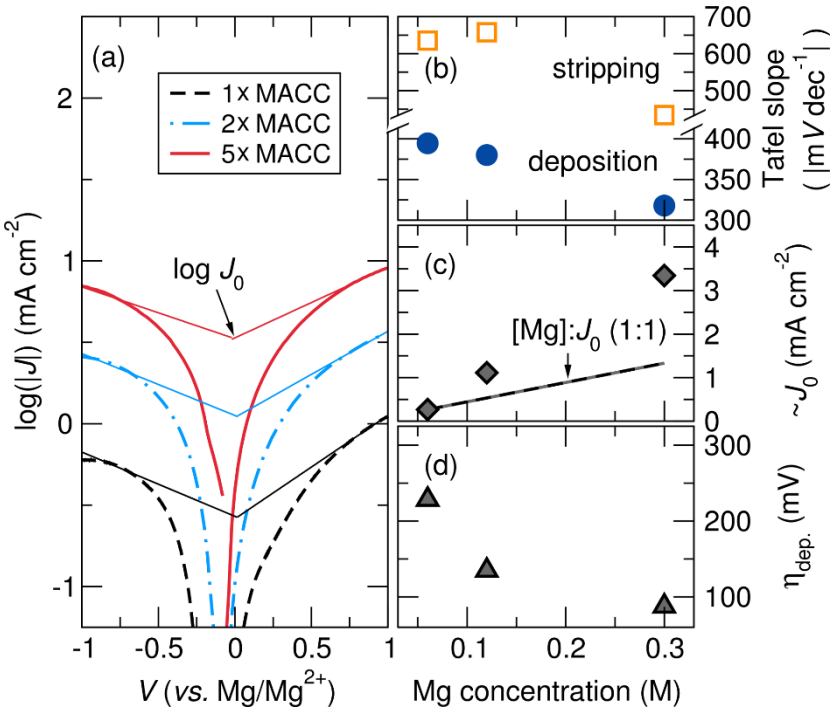

Figure S3. Mg deposition and stripping in the MACC electrolyte at various concentrations. 1× MACC is defined as 30 mM $AlCl_3$ + 60 mM $MgCl_2$. The indicated values are obtained by cycling the conditioned MACC electrolytes with a Pt working electrode and Mg counter/reference from -1.2 V to 2.8 V at 5 mV s^{-1}. (a) Tafel plots for the deposition and stripping of Mg. (b) The Tafel slopes for deposition and stripping and (c) the exchange current density, J_0, for each electrolyte concentration obtained from fitting the linear regions in (a). We note, however, that it is difficult to determine the actual J_0 from macroelectrodes and these numbers should only be considered to compare the three electrolyte concentrations. (d) The deposition overpotential as a function of Mg concentration.

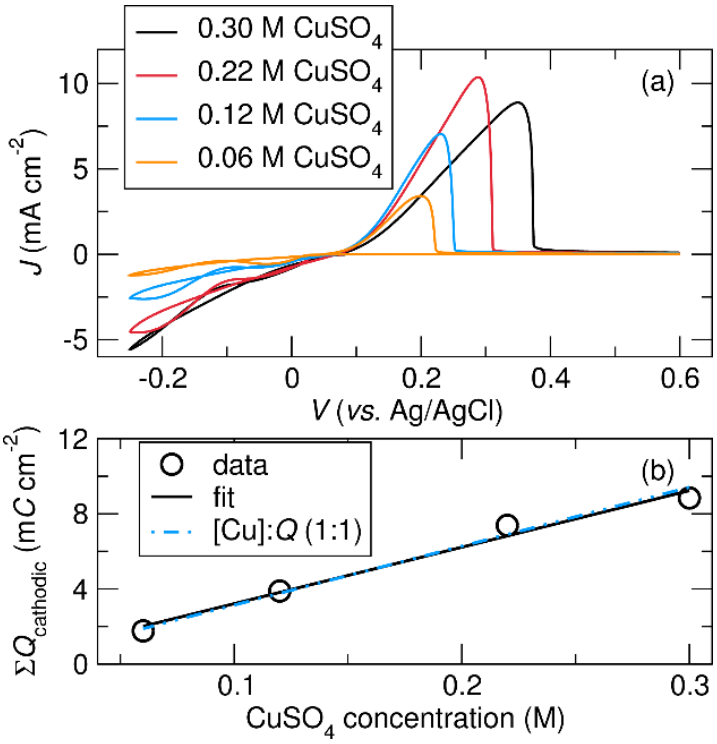

Figure S4. (a) Cyclic voltammograms showing Cu^{2+} electrodeposition and stripping of an electrolyte consisting of 0.4 M H_2SO_4 with varied concentrations of $CuSO_4$. The cell consists of a 5 mm glassy carbon working electrode, Cu counter electrode, and Ag/AgCl reference electrode. The CVs are measured at 5 mV s^{-1} from -0.26 V (vs. Ag/AgCl) to 0.6 V (vs. Ag/AgCl). The Coulombic efficiency is 96.6%, 96.9%, 95.7%, and 94.2% for the 0.30 M, 0.22 M, 0.12 M, and 0.06 M electrolytes, respectively. (b) The corresponding sum of the cathodic charge passed for each concentration along with the linear fit. The correlation between the total charge passed and the Cu^{2+} concentration is very close to 1:1. The line showing $[Cu^{2+}]$:Q at 1:1 is extrapolated from the $\Sigma Q_{cathodic}$ in the 0.06 M $CuSO_4$ electrolyte.

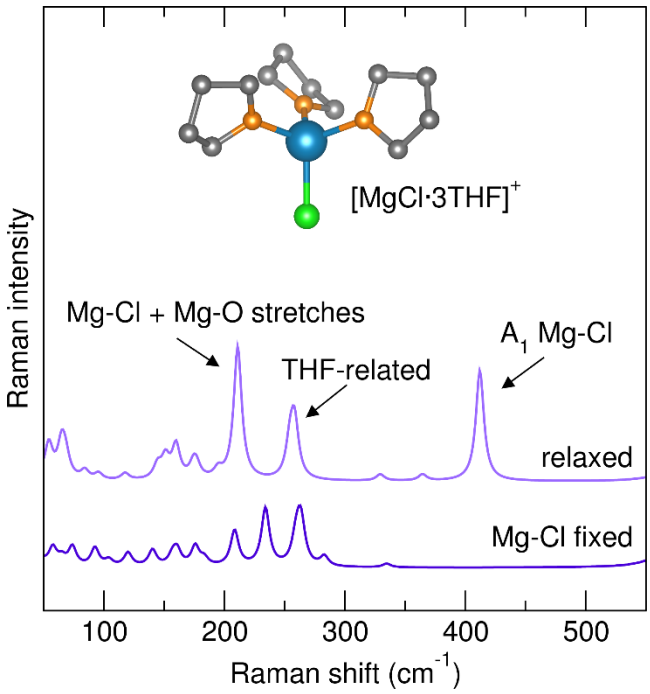

Figure S5. Simulated Raman spectra of the four-coordinate Mg monomer $[MgCl·3THF]^+$. The Mg–Cl and Mg–O fixed spectrum is not shown as the structure was unable to be converged.

Table S1. Lorentzian fit values of ^{35}Cl NMR

	high frequency peak			low frequency peak		
	chemical shift (ppm)	FWHM (MHz)	area (rel. %)	chemical shift (ppm)	FWHM (MHz)	area (rel. %)
0.06 M $AlCl_3$	40	8599	100	--	--	--
2× MACC as-prepared	60	4042	57.1	4	7570	42.9
2× MACC conditioned	50	3380	32.6	-12	4777	67.4
0.015 M$AlCl_3$	45	8379	100	--	--	--
5× MACC as-prepared	55	3969	100	--	--	--
5× MACC conditioned	50	4042	51.3	-5	3969	48.7

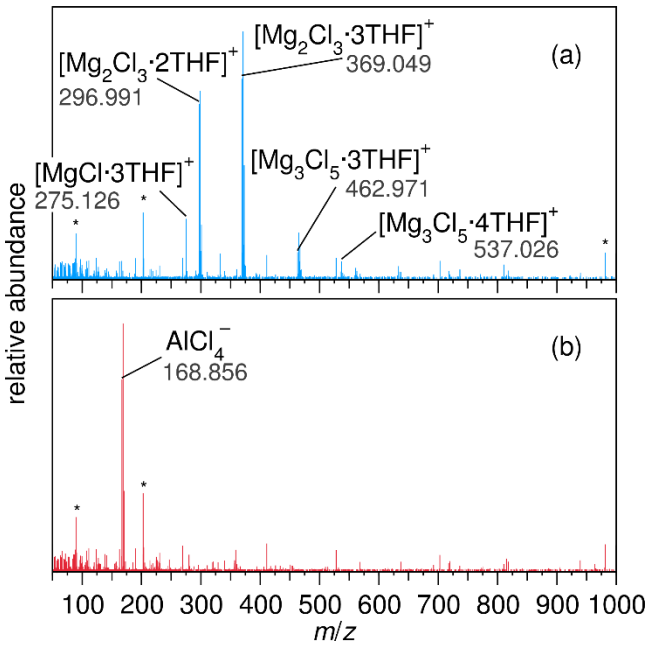

Figure S6. Sonic spray ionization mass spectrometry of the conditioned 1× MACC in (a) positive ion mode and (b) negative ion mode. The peaks marked with "*" are impurities present in the instrument.

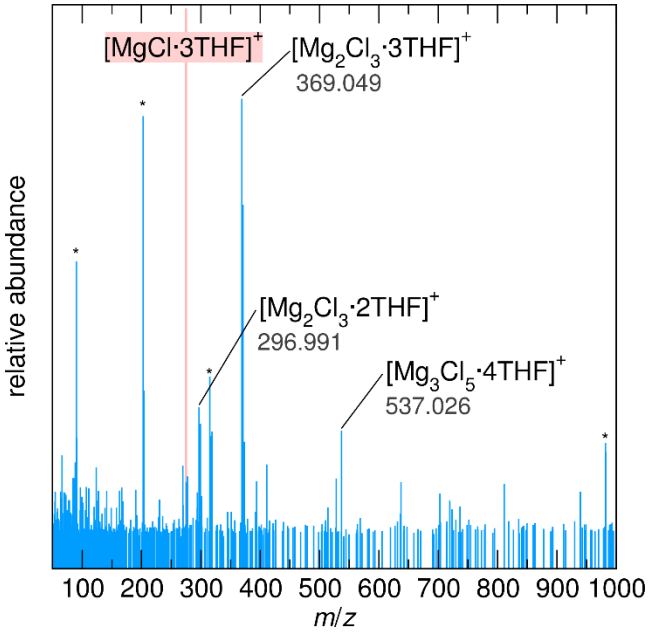

Figure S7. Sonic spray ionization mass spectrometry of conditioned 5× MACC in positive ion mode. The peaks marked with "*" are impurities present in the instrument.